

This item is the archived peer-reviewed author-version of:

Stand age and species richness dampen interannual variation of ecosystem-level photosynthetic capacity

Reference:

Musavi Talie, Migliavacca Mirco, Reichstein Markus, Kattge Jens, Wirth Christian, Black T. Andrew, Janssens Ivan, Knohl Alexander, Loustau Denis, Rouspard Olivier,- Stand age and species richness dampen interannual variation of ecosystem-level photosynthetic capacity
Nature Ecology & Evolution - ISSN 2397-334X - 1:2(2017), UNSP 0048
Full text (Publisher's DOI): <https://doi.org/doi:10.1038/S41559-016-0048>
To cite this reference: <http://hdl.handle.net/10067/1486030151162165141>



Stand age and species richness dampen interannual variation of ecosystem-level photosynthetic capacity

Postprint version

Musavi, T., Migliavacca, M., Reichstein, M., Kattge, J., Wirth, C., Black, T. A., Ivan Janssens, Alexander Knohl, Denis Loustau, Olivier Roupsard, Andrej Varlagin, Serge Rambal, Alessandro Cescatti, Damiano Gianelle, Hiroaki Kondo, Rijan Tamrakar and Miguel D. Mahecha

Published in: **Nature Ecology & Evolution**

Reference: Musavi, T., Migliavacca, M., Reichstein, M., Kattge, J., Wirth, C., Black, T. A., et al. (2017). Stand age and species richness dampen interannual variation of ecosystem-level photosynthetic capacity. *Nature Ecology & Evolution*, 1: 0048. doi:10.1038/s41559-016-0048.

Web link: <https://www.nature.com/articles/s41559-016-0048>



This project has received funding from the European Union's Horizon 2020 research and innovation programme under grant agreement No 640176

Stand age and species richness dampen interannual variation of ecosystem-level photosynthetic capacity

Talie Musavi^{1*}, Mirco Migliavacca¹, Markus Reichstein^{1,2}, Jens Kattge^{1,2}, Christian Wirth^{2,3}, T. Andrew Black⁴, Ivan Janssens⁵, Alexander Knohl⁶, Denis Loustau⁷, Olivier Roupsard⁸, Andrej Varlagin⁹, Serge Rambal^{10,11}, Alessandro Cescatti¹², Damiano Gianelle^{13,14}, Hiroaki Kondo¹⁵, Rijan Tamrakar⁶ and Miguel D. Mahecha^{1,2}

The total uptake of carbon dioxide by ecosystems via photosynthesis (gross primary productivity, GPP) is the largest flux in the global carbon cycle. A key ecosystem functional property determining GPP is the photosynthetic capacity at light saturation (GPP_{sat}), and its interannual variability (IAV) is propagated to the net land-atmosphere exchange of CO_2 . Given the importance of understanding the IAV in CO_2 fluxes for improving the predictability of the global carbon cycle, we have tested a range of alternative hypotheses to identify potential drivers of the magnitude of IAV in GPP_{sat} in forest ecosystems. Our results show that while the IAV in GPP_{sat} within sites is closely related to air temperature and soil water availability fluctuations, the magnitude of IAV in GPP_{sat} is related to stand age and biodiversity ($R^2 = 0.55$, $P < 0.0001$). We find that the IAV of GPP_{sat} is greatly reduced in older and more diverse forests, and is higher in younger forests with few dominant species. Older and more diverse forests seem to dampen the effect of climate variability on the carbon cycle irrespective of forest type. Preserving old forests and their diversity would therefore be beneficial in reducing the effect of climate variability on Earth's forest ecosystems.

Interannual variability (IAV) of the net carbon dioxide exchange over land is globally the main determinant of the variability of atmospheric CO_2 growth rate^{1,2}. So understanding the factors controlling the IAV in CO_2 fluxes is essential to improve the predictability of the global carbon cycle³. Ecosystem biotic properties — such as soil and canopy nutrient status, rates of change in physiological properties of the vegetation, or the sensitivity of these properties to environmental factors — influence ecosystem CO_2 exchange. Recent studies have shown that the IAV of the carbon budget can be better explained by variation in biotic properties of ecosystems such as photosynthetic capacity (GPP_{sat}) than directly by environmental and climatic drivers^{4–6}. GPP_{sat} is defined as the value of gross primary productivity (GPP) at saturating light under non-stressed conditions, minimizing the influence of anomalous hydrometeorological conditions (for example, droughts and heatwaves), which potentially affect photosynthesis. A robustly retrieved characterization of GPP_{sat} can be regarded as an ecosystem functional property reflecting the physiological response of the ecosystem to the environment. Given that IAV of GPP_{sat} must propagate to observed GPP, this quantity is thought to be a key variable in understanding IAV of carbon fluxes⁷. In fact, recent studies demonstrated that GPP_{sat} correlates more strongly than any climatic variable with

annual GPP⁸, but also correlates with net ecosystem CO_2 exchange⁵. The magnitude of IAV in GPP_{sat} has been shown to exhibit considerable variation across ecosystems⁹, yet no obvious explanation for this pattern has been reported in the literature. However, the consequences are important: a low IAV in GPP_{sat} would suggest that ecosystem functioning is not very sensitive to climatic variability, and that it preserves its functionality under the influence of that variability — and, likewise, high IAV is a consequence of high sensitivity. The capability of an ecosystem to preserve its functioning and structure over time (after external disturbances or climate extremes), is often defined as ecosystem stability and is linked to ecosystem resilience¹⁰. Using this terminology, low values of IAV in GPP_{sat} can be understood as a characterization of high ecosystem functional stability.

The relation of ecosystem functionality, structure and stability has been a matter of debate for many decades in the field of ecology. In particular, the diversity of vascular plants has been investigated as a stabilizing factor with respect to variations in productivity, for example by buffering the ecosystem's sensitivity to climate extremes¹¹. However, it is also well known that plant diversity is co-limited by soil properties¹², ecosystem management, and climate conditions. Another variable to consider is stand age

¹Max Planck Institute for Biogeochemistry, 07745 Jena, Germany. ²German Centre for Integrative Biodiversity Research (iDiv) Halle-Jena-Leipzig, 04103 Leipzig, Germany. ³Institute of Special Botany and Functional Biodiversity, University of Leipzig, 04103 Leipzig, Germany. ⁴Biometeorology and Soil Physics Group, Faculty of Land and Food Systems, University of British Columbia, 2329 West Mall, Vancouver, British Columbia, Canada. ⁵University of Antwerpen, Department of Biology, 2610 Wilrijk, Belgium. ⁶Bioclimatology, Georg-August University of Göttingen, 37077 Göttingen, Germany. ⁷INRA, ISPA, Centre de Bordeaux Aquitaine, 71 Avenue Edouard Bourlaux, 33140 Villenave-d'Ornon, France. ⁸UMR Ecologie Fonctionnelle and Biogéochimie des Sols et Agroécosystèmes, SupAgro-CIRAD-INRA-IRD, Montpellier, France. ⁹A.N. Severtsov Institute of Ecology and Evolution, Russian Academy of Sciences, Moscow, 119071, Russia. ¹⁰Centre d'Ecologie Fonctionnelle et Evolutive, CEFV, UMR 5175, CNRS, Montpellier, France. ¹¹Universidade Federal de Lavras, Lavras, MG, 37200-000, Brazil. ¹²European Commission, Joint Research Centre, Directorate for Sustainable Resources, 21027, Ispra, Italy. ¹³Department of Sustainable Agro-Ecosystems and Bioresources, Research and Innovation Center, Fondazione Edmund Mach, 38010 San Michele all'Adige Trento, Italy. ¹⁴Foxlab Joint CNR-FEM Initiative, Via E. Mach 1, 38010 San Michele all'Adige, Italy. ¹⁵National Institute of Advanced Industrial Science and Technology (AIST), Onogawa, Tsukuba, Ibaraki, 305-8561, Japan. *e-mail: tmusavi@bgc-jena.mpg.de

Table 1 | Summary of the linear models fitted for $cvGPP_{sat}$ (the interannual variability of ecosystem photosynthetic capacity computed for each FLUXNET site) with the chosen predictors for the different groups of sites classified according to vegetation type.

Sites PFT	R^2	adj. R^2	Predictors	Coefficients	s.e.	d.f.	P
DBMF	0.65	0.60	Intercept	0.38	0.05	13	<0.0001
			ln(Age)	-0.06	0.01		0.0004
			Sp. no.	-0.01	0.00		0.02
DBMF	0.46	0.42	Intercept	0.31	0.05	14	<0.0001
			ln(Age)	-0.05	0.01		0.004
			Sp. no.	-0.02	0.007		0.02
EF	0.49	0.46	Intercept	0.38	0.04	31	<0.0001
			ln(Age)	-0.05	0.01		<0.0001
			Sp. no.	-0.02	0.007		0.02
EF	0.40	0.38	Intercept	0.35	0.05	32	<0.0001
			ln(Age)	-0.05	0.01		<0.0001

PFT, plant functional types; s.e., standard error; d.f., degree of freedom; DBMF, deciduous broad leaf and mixed forests; EF, evergreen forests. ln(Age) is the natural logarithm of the average stand age, and sp. no. is the number of dominant plant species that have a cumulative abundance of 90% at the sites.

(the mean age of the forest stand or the number of years after a major stand replacement after disturbance), which may affect ecosystem stability through adaptation, particularly of trees to their environment — hence increasing ecosystem resilience to climate variability¹³. Moreover, structural parameters such as canopy cover, rooting depth, canopy height or leaf area index (LAI), which also depend on tree species diversity and stand age¹⁴, have an important effect on the ecosystem response to variation in environmental drivers since they define the capacity of trees to access resources such as water and light¹⁵. For instance, a regional study in the Amazon basin has shown that GPP, derived from the remotely sensed enhanced vegetation index, is less sensitive to environmental influences in regions with high canopy cover¹⁶.

Despite this growing body of ecological knowledge, it remains largely uncertain which factors stabilize ecosystem functional

properties at the global scale. In particular, we do not understand the causes of variability of specific ecosystem functional properties, such as photosynthetic capacity across ecosystem types, which ultimately controls ecosystem productivity. Here we hypothesize that stand age and species diversity play an important role in stabilizing ecosystem photosynthetic capacity. We test this hypothesis while also considering other factors related to climate, water availability, forest structure and soil properties that might have direct or indirect effects on ecosystem photosynthetic capacity.

In this study, we used measurements of ecosystem-level fluxes, and climate variables (temperature, precipitation, and water availability), species richness, stand age, forest structure (canopy cover, height, and LAI), and soil properties (nutrient availability¹⁷) derived from satellite data, *in situ* observations and the literature (see the Methods).

We used half-hourly ecosystem-level GPP fluxes estimated by the means of the eddy-covariance technique at 50 FLUXNET sites¹⁸ with at least 4 years of measured fluxes, and with different vegetation types across different climatic regions. We included data from evergreen forest (EF) as well as deciduous broadleaved and mixed forest (DBMF) located in temperate, boreal, mediterranean, tropical and dry climate regions (Supplementary Fig. 1 and Table 1). All 50 sites have information on stand age (referred to simply as ‘age’ in Figs 1–3) and species richness in addition to the CO₂ flux data. Species richness (‘sp. no.’ in Figs 1–3) is the number of dominant plant species (for example tree or herb) that account for a cumulative abundance of 90 percent at a given site. We collected additional information on (i) canopy cover, (ii) canopy height, (iii) LAI, (iv) temperature and precipitation, and (v) soil water availability index (WAI) for a subset of 44 sites; and (vi) an index of nutrient availability for 36 sites compiled from the literature¹⁷ (see Methods).

We characterized the response of half-hourly GPP estimates to incoming shortwave radiation by fitting ecosystem-level light response curves yielding daily estimates of GPP_{sat} (see Methods). The site-level estimates of annual GPP_{sat} (that is, GPP at saturating light conditions) were then determined by extracting the 90th percentile of the daily estimates of GPP_{sat} . The magnitude of the IAV in GPP_{sat} was computed as the coefficient of variation of annual estimates of GPP_{sat} ($cvGPP_{sat} = \sigma(GPP_{sat}(t))/\mu(GPP_{sat}(t))$), where $GPP_{sat}(t)$ is the annual GPP_{sat} for year t , and σ and μ are the standard deviation and mean of $GPP_{sat}(t)$, respectively. Two variable selection methods based on (i) relative importance of regressors

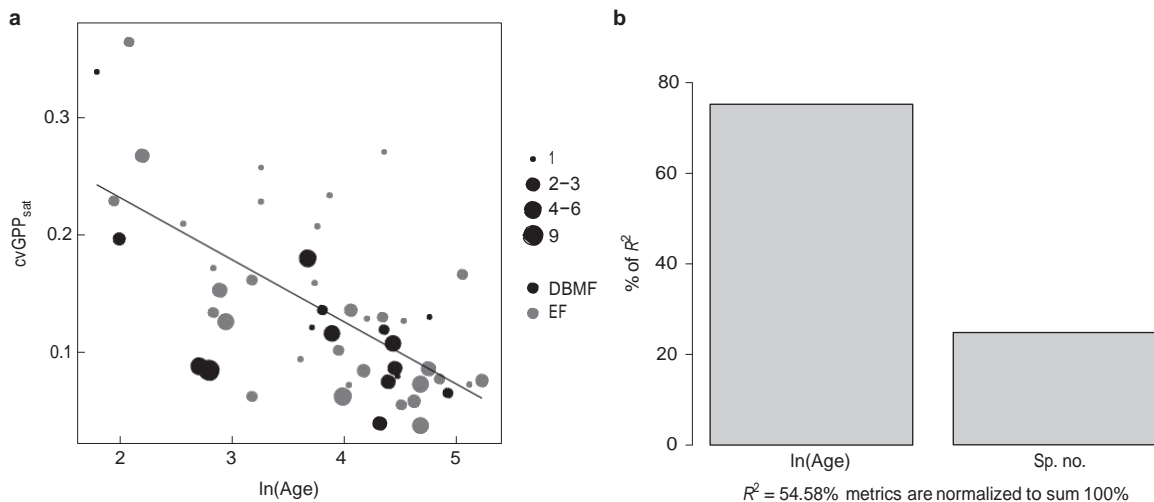


Figure 1 | relationship of $cvGPP_{sat}$ with stand age and species richness. **a**, The relationship between the interannual variability of ecosystem photosynthetic capacity ($cvGPP_{sat}$) computed for each FLUXNET site and stand age (which is transformed using the natural logarithm, ln(age)): ($R^2 = 0.39$, $P < 0.0001$, $n = 50$). The number of plant species at the sites that account for 90% of the total species abundances (sp. no.) is indicated with the size of the points. DBMF, deciduous broad leaf and mixed forests ($n = 16$; black); EF, evergreen needleleaf and broadleaf forests ($n = 34$; grey). **b**, Relative importance metrics of ln(age) and sp. no. as predictors of $cvGPP_{sat}$. For a version of this figure using age without logarithm transformation, see Supplementary Fig. 11.

Table 2 | Comparison of different models computed using the set of predictors chosen by both stepwise model selection according to aIC and relative importance methods.

Model structure	R^2	adj. R^2	Predictors	Coefficients	P
cvGPP _{sat} ~ sp. no.	0.12	0.10	Intercept Sp. no.	0.18 ± 0.02 −0.01 ± 0.00	0.01
cvGPP _{sat} ~ age	0.25	0.24	Intercept Age	0.19 ± 0.01 −0.00 ± 0.00	0.0002
cvGPP _{sat} ~ ln(age)	0.39	0.38	Intercept ln(Age)	0.33 ± 0.04 −0.05 ± 0.01	<0.0001
cvGPP _{sat} ~ ln(age) + sp. no.	0.55	0.53	Intercept ln(Age) Sp. no.	0.39 ± 0.03 −0.05 ± 0.01 −0.02 ± 0.00	<0.0001
cvGPP _{sat} ~ ln(age) + sp. no. + age:sp. no.	0.55	0.52	Intercept ln(Age) Sp. no. ln(Age):sp. no.	0.42 ± 0.06 −0.06 ± 0.01 −0.03 ± 0.02 0.00 ± 0.00	<0.0001

cvGPP_{sat} is the IAV magnitude of ecosystem photosynthetic capacity, and sp. no. is the number of dominant plant species that have a cumulative abundance of 90% at the sites. ln(Age) is the natural logarithm of the average stand age. The number of sites is $n = 50$.

(Gromping *et al.*, 2006)¹⁹, and (ii) multivariate generalized regression models and a stepwise algorithm based on Akaike Information Criteria (stepAIC) were used to select the most relevant predictors of the IAV of GPP_{sat} (see Methods).

Results

Results from the variable selection and relative importance methods (see Methods) conducted over the 44 sites with all variables are consistent with our hypothesis that stand age and species richness of the sites are the most important predictors of cvGPP_{sat}, with stand age being statistically the dominant factor (Fig. 1a). We further tested the performance of a multiple linear model, where cvGPP_{sat} is a function of stand age and species richness, using all sites with data available for these two predictors (50 sites). The model suggests

a clear relationship between cvGPP_{sat} and the logarithm of stand age and the species richness (Table 2, $R^2 = 0.55$, $P < 0.0001$). Stand age, which is negatively correlated with cvGPP_{sat}, is the most important predictor (from the 55% explained variance by both variables, the relative contribution to the explained variance by stand age and species richness is 74.5% and 25.5%, respectively; Fig. 1b and Supplementary Fig. 2). The relationship between cvGPP_{sat} and stand age also holds across the different forest types (ENF and DBMF) (Fig. 1a and Table 1). Species richness has a complementary effect: for the same age class, higher values of species richness yield lower IAVs of GPP_{sat} (Table 2 and Fig. 1a). While species richness has a negative relation with cvGPP_{sat} (Fig. 2a and Table 2), it is not correlated with stand age ($R^2 = 0$, Fig. 2b). Furthermore, Fig. 1 shows that the slope of cvGPP_{sat} versus stand age is similar for the two different forest types, which suggests that the relationship between cvGPP_{sat} and stand age is independent of forest type (Table 1). The relationship is also independent of LAI_{max} of the sites (Supplementary Fig. 3). In young forests, cvGPP_{sat} might depend also on the expected trend in annual growth and GPP, as young stands are expected to rapidly increase their biomass and LAI in the first years of establishment²⁰. Thus, young stands could have a higher variability of GPP_{sat} — but this does not necessarily reflect instability. To remove this potentially confounding factor, we tested whether there is a temporal trend in our data of annual GPP_{sat} at the sites (Methods). Using a Mann-Kendall test, we found only five sites had a significant trend, two of which were old sites (>80 years). The results of the model selection and the relationship between cvGPP_{sat}, stand age and species richness remains the same regardless of whether the trend in GPP_{sat} from these sites is removed (see Supplementary Information).

While there is a strong relationship between the annual GPP_{sat} and mean growing season temperature and WAI (Fig. 3 and Supplementary Figs 4–7) across all sites, the magnitude of the IAV of GPP_{sat} is best explained by stand age differences, and not by the differences in the IAV of climate and environmental factors (that is, standard deviation of annual growing season temperature and WAI). The distance correlation coefficient between GPP_{sat} and climate variables, which can account for nonlinearity in statistical relations, is also not linked to stand age, species richness or cvGPP_{sat} (Supplementary Fig. 8). Pairwise relationships between cvGPP_{sat}, environmental variables and ecosystem structural variables were also tested. Soil nutrient availability has no effect on the

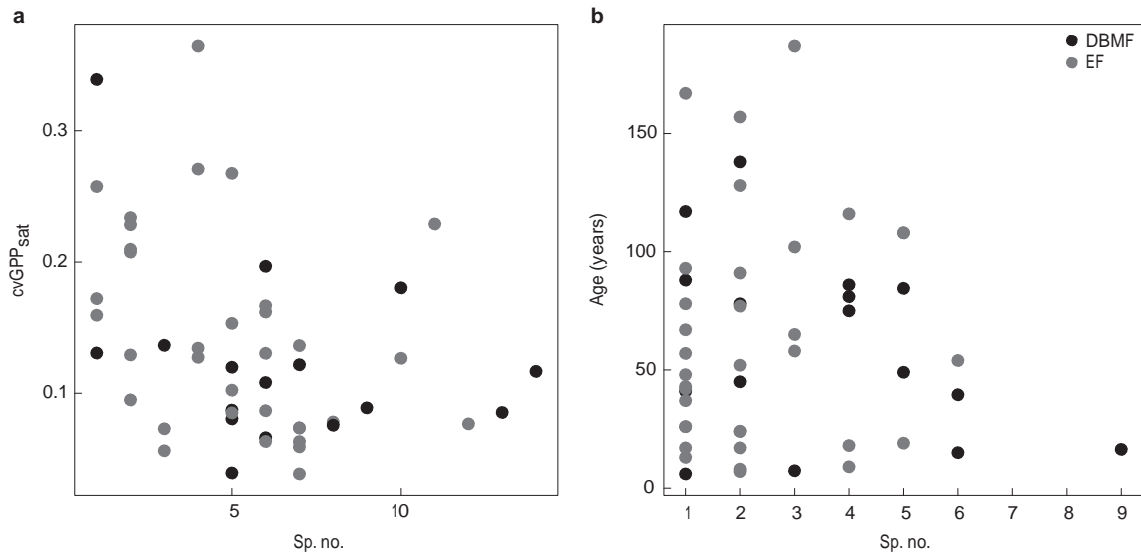


Figure 2 | Relationship of species richness with stand age and cvGPP_{sat}. **a**, The relationship between cvGPP_{sat} computed for each FLUXNET site and species richness (sp. no.) ($R^2 = 0.12$, $P = 0.01$, $n = 50$). **b**, The relationship between species richness and stand age ($R^2 = 0$, $P = 0.68$, $n = 50$). DBMF are deciduous broad leaf and mixed forests ($n = 16$; black) and EF are evergreen needleleaf and broadleaf forests ($n = 34$; grey).

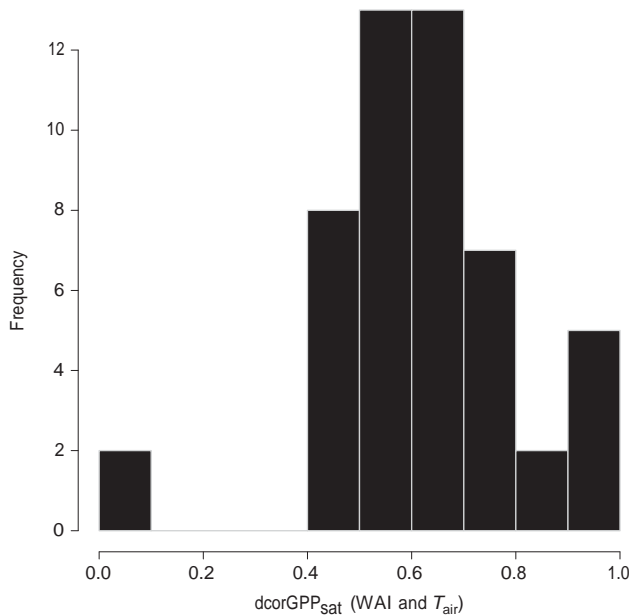


Figure 3 | Frequency distribution of the distance correlation coefficients computed between the annual ecosystem photosynthetic capacity (GPP_{sat}) and the environmental variables W_{ai} and T_{air} ($n=50$). W_{ai} , average water availability index; and T_{air} , temperature (both during the growing season). Using the distance correlation coefficient ($dcor$)³², we show the strength of the correlation of GPP_{sat} with W_{ai} and T_{air} jointly (see the Methods).

$cvGPP_{sat}$ (Supplementary Fig. 9), and neither do the other variables (Supplementary Fig. 10).

Discussion

Previous studies have shown that vegetation responses to climate variability can explain the IAV of ecosystem fluxes better than climate variables themselves on longer timescales^{4,6,21}. Here we show further that the magnitude of IAV in GPP_{sat} (ecosystem photosynthetic capacity) is best explained by vegetation properties of the sites. We identify a joint control of stand age and biodiversity on the magnitude of the IAV of ecosystem photosynthetic capacity (that is, $cvGPP_{sat}$). Part of the unexplained variance in $cvGPP_{sat}$ by stand age and species richness could be also associated with management and disturbances that were not included in the ancillary database of the sites, and can therefore not be formally investigated. Accurately simulating GPP in terrestrial biosphere models depends crucially on parameters related to GPP_{sat} ²². These parameters are typically assumed to be constant over time, but may vary spatially according to forest types²³. Our findings suggest that stand age and species richness should be accounted for to dynamically adjust parameters related to photosynthetic capacity.

Stand age can influence GPP_{sat} stability in different ways by enhancing soil conditions over time (for example, a thicker humus layer with favourable microbial communities, increased water storage capacity, and access to deeper water with a tap root system¹³). Also, a forest may develop a more diverse canopy and rooting structure, allowing for more complementary use of nutrients and water. In addition, older forests are more resilient to environmental changes because with time species selection leads to a better adaptation to the environment²⁴. Site fertility can also improve with stand age, following the nutrient losses occurring during major disturbances (such as fire or harvest). In fact, the ecosystem internal cycle of macronutrients is particularly relevant^{25,26} and leads to a progressive accumulation of nutrients in the living biomass with age²⁷.

Although species diversity is generally assumed to increase ecosystem resilience, exceptions have been reported²⁸. For example, species diversity can enhance forest resistance to drought only if the system is prone to drought²⁸. This is considering the gradual adaptation of the ecosystem to its environment by changing species composition to track environmental changes. Facilitation (species interactions that results in the species benefitting from each other) and complementary functioning of plant species can explain why species richness is important for ecosystem stability and how the interaction of species modulates the climate effect on ecosystem functioning²⁹. In addition, mixed forests are able to buffer the effect of climate IAV through competition and facilitation in normal and stressful years, respectively²⁹. Facilitation and complementary effects are clearly related to the functional richness of the species pool (that is, species with different functional traits), which is linked to stand age as shown by a regional study in the tropics³⁰. Diverse ecosystems with a higher number of plant species respond less dramatically in their functioning (compared to ecosystems with single or few species) to climate and environmental stresses.

The Earth's forest cover is essential to remove CO_2 from the atmosphere, and afforestation is important to compensate for forest loss due to land use changes (such as agriculture). While young forests established on former agricultural lands, or burned and harvested forests for several years cannot compensate for the initial carbon loss nor contribute to CO_2 sequestration from the atmosphere, old forest stands retain their capacity to sequester CO_2 for long periods^{31,32}. We show that the photosynthetic capacity and therefore the gross primary production of old growth forests are more resilient to climate variability than young forests. In addition, our study suggests that species-rich forest stands offer a larger potential for maintaining a stable photosynthetic capacity across time than species-poorer stands. Therefore, preserving our current forest (with old forests covering 15% of Earth's surface³²) and their species diversity may attenuate the annual fluctuations of global forest-atmosphere CO_2 exchange.

Methods

Data. In this study we brought together a wide range of data: ecosystem-atmosphere CO_2 fluxes measured at eddy covariance flux sites, information about climate (temperature, precipitation, and water availability index (WAI)), species richness, stand age, and plant traits, derived from field campaigns, and information about forest structure derived from satellite data for each of the selected sites; finally, data about nutrient availability was derived from the literature¹⁷. Sites were selected according to the availability of eddy covariance flux measurements for at least 4 years, information about stand age, canopy cover, canopy height, and species abundance. This led to a global dataset of 50 sites with different vegetation types across different climatic regions. We included data from evergreen forest (EF) and deciduous broadleaved and mixed forest (DBMF) located in temperate, boreal, tropical, Mediterranean and dry climate regions.

CO_2 fluxes and meteorological data. From the global eddy covariance flux database¹⁸ we downloaded half-hourly ecosystem-level gross primary productivity (GPP) fluxes estimated from net ecosystem exchange (NEE) data³⁴. Half-hourly shortwave incoming global radiation, temperature, and precipitation were also downloaded. From the dataset WAI was computed according to ref. ³⁵. Here the WAI is the ratio between soil water storage and plant available water storage capacity at lower layer (100 mm)³⁵.

Average stand age. These data were obtained from the Biological, Ancillary, Disturbance and Metadata (BADM) of the FLUXNET database³⁶. Stand age (expressed in years) reported in the BADM is the average tree age of the stand or the age of the stand since the last major disturbance that caused stand replacement. Stand age was reported for different years at the sites, and so we normalized the data by using the age of all sites at the year 2007 (which is the year of the release of FLUXNET LaThuile Database used in this study).

Species richness. Species identity and abundances from the BADM data and literature search were collected. Because these data come from diverse sources and are collected with different protocols, they can have variable level of details. Therefore, we developed a strategy to guarantee comparability of the plant species richness computed across sites. For each site we sorted the plant species according to their

abundance, from the one with highest abundance to the lowest. Then we considered only the number of species that add up to 90% of the total site abundance.

Canopy structure. For the selected sites we extracted satellite products to characterize canopy structure: canopy cover, plant height and Leaf Area Index (LAI).

Canopy cover was extracted from the Moderate Resolution Imaging Spectroradiometer (MODIS) vegetation products continuous field version 4³⁷ (<http://glcf.umd.edu/data/vcf/>).

Plant height was derived for each site from the estimates reported in ref. ³⁸ (<http://lidarradar.jpl.nasa.gov/>).

We used estimates of LAI derived at 1 km (0.01°) spatial resolution by the JRC-TIP³⁹ from the MODIS broadband visible and near-infrared surface albedo products⁴⁰. The processing for the gap filling and the extraction of the time series from MODIS-TIP LAI products is described in ref. ⁹. Annual maximum LAI values were derived at each site by extracting for each year the 90th percentile of the 16-day LAI time series. Finally for each site the maximum LAI (LAI_{max}) and the coefficient of variation of the annual maximum LAI (cvLAI_{max}) were estimated. In this study we did not use site level LAI data reported in the FLUXNET database for the following reasons:

1. LAI data have been collected with a variety of different methods, from direct (that is, harvesting and litter fall) to indirect (for example, hemispherical photography or LAI-2000) methods. Site-level method intercomparisons of various techniques always reveal large and non-systematic differences among LAI methodologies, rendering the LAI information reported in the FLUXNET database not always suited for network synthesis studies. Efforts toward the standardization of the collection of these measurements are ongoing in the context of the Integrated Carbon Observation System (ICOS) and National Ecological Observatory Network (NEON), but these data are not yet available.
2. The availability of data in regular annual measurement is very different among sites. For some sites the LAI is available for each measurement year (and sometimes even seasonally), but for many sites only one estimate during the whole measurement period is available.

Considering the limitations of site-level LAI data, we selected the MODIS-TIP LAI product. MODIS-TIP LAI is recognized as one of the most effective LAI products available and it was successfully evaluated at a FLUXNET site included in this study⁴¹.

Nutrient availability. Part of the dataset (36 sites) was complemented with soil nutrient availability classes derived from literature¹⁷. For each site, nutrient availability was computed using site-level specific information about the following variables: carbon, nitrogen and phosphorus concentrations of soil and/or leaves, soil type, soil texture, soil C/N ratio, and soil pH. These data were derived for each site from the literature and in some cases provided by the site principal investigator. The sites were eventually classified in three classes: low, medium and high nutrient availability. Afterwards the classification was approved by the site principal investigators¹⁷.

Estimation of photosynthetic capacity and its interannual variability

magnitude. Site-level estimates of the annual photosynthetic capacity (GPP_{sat}) were determined from half-hourly GPP estimates and global solar radiation (Rg)⁹.

In summary, we fit a non-rectangular hyperbolic light response curve (NHLRC) to GPP and Rg data⁴². The NHLRC was fit to 5 days of data selected with a moving window approach. The parameters of the NHLRC were estimated and we computed the GPP at 1,000 W m⁻² of Rg (GPP_{1,000}), which represents the GPP at saturating light (that is, ecosystem photosynthetic capacity in the selected 5-day window). The estimated parameters and the GPP_{1,000} values were assigned to the day in the middle of the 5-day window. Parameters estimated with R² of the fitting lower than 0.6 were removed.

To estimate the annual GPP_{sat} for each year from the daily GPP_{1,000} time series, we calculated the 90th percentile. The interannual variability (IAV) of the annual estimates of GPP_{sat} was computed as the coefficient of variation of GPP_{sat}, that is, cvGPP_{sat}, calculated by dividing the standard deviation by the mean

$$\left(\frac{\text{standard deviation}}{\text{mean}} \right)$$

In young stands cvGPP_{sat} might depend on the trend in annual growth and GPP that can lead to high cvGPP_{sat} values that are not related to interannual variability in photosynthetic capacity. To remove this confounding factor we first tested the presence of a significant trend in GPP_{sat} time series at each site with the Mann-Kendall non-parametric trend test. Finally, for the sites with a significant trend ($P < 0.1$) we recomputed the cvGPP_{sat} by detrending the GPP_{sat} time series (that is, the standard deviation of detrended GPP_{sat} divided by the mean of the GPP_{sat}, hereafter referred as detrended cvGPP_{sat}).

Aggregation of environmental variables: For the estimation of year-to-year variability of climate we used temperature and precipitation measured, and the WAI¹⁵ estimated at the flux sites. To aggregate temperature and precipitation we used only daily values with more than 70% of original half-hourly data (gaps in

the half-hourly data are filled using ERA-Interim climate data downscaled at the FLUXNET, <http://www.bgc-jena.mpg.de/~MDIwork/meteo/index.php>). Average temperature, WAI, and cumulative precipitation over the active growing season were computed. Active growing season was considered as the days with daily GPP higher than the annual median GPP. From these annual estimates we derived the standard deviation (s.d.) of annual mean temperature, WAI and precipitation during the growing season as a measure of their IAV.

Statistical analysis. We used a variable selection method and relative importance method to select and quantify the contribution of each predictor (for example, average stand age (age), ln(age), species richness (sp. no.), canopy cover, canopy height, and nutrient availability, temperature, WAI) to the cvGPP_{sat}; precipitation was once used in the calculation instead of WAI.

The stepwise algorithm based on the Akaike Information Criteria (AIC) algorithm with generalized linear regression models was used⁴³. The independent variable was cvGPP_{sat}, while the predictors were stand age (referred to in the figures simply as 'age'), species abundance (sp. no.), ln(age), s.d. of temperature and of WAI, canopy cover, canopy height, LAI, and so on; interactions of age and sp. no., s.d. of temperature and s.d. of WAI and canopy height and LAI_{max} were also included (cumulative precipitation was also used in place of WAI with similar results; data not shown). The algorithm was set up with the possibility to account for model pairwise interactions, and imposing a selection only if the model is statistically significant ($P < 0.01$). Although the sites used in this study have at least 4 years of flux data, the number of years (no.years) with available data at each site was different. Therefore, we used

$$\frac{1}{\sqrt{\text{no. years}}}$$

to weight the model selection, weighting more the sites with higher numbers of years. A stepwise selection without the weighting was used as well. The distribution of the residuals of the best model was tested for normality using the Shapiro and Kolmogorov-Smirnov test. The results showed that the residuals were normally distributed; therefore the weighting was not strictly necessary, but was used for a comprehensive evaluation.

In order to assess the uncertainty introduced by the potential trend in GPP_{sat} in young stands, we repeated the analysis using the detrended cvGPP_{sat} dataset, and the cvGPP_{sat} for the sites without a significant trend in GPP_{sat}.

To disentangle the importance of each predictor in determining cvGPP_{sat} we used the Lindeman-Merenda-Gold (LMG) relative importance method⁴⁹. This method allows the assessment of the importance of correlated predictors in a multiple linear regression model. Moreover, the pairwise linear regression and correlation between the different predictors and cvGPP_{sat}, and between the predictors themselves, was tested.

Both stepwise AIC and the LMG identified ln(age) and sp. no. as the most important variables controlling the cvGPP_{sat}. We used a generalized linear model to fit the coefficients of the multiple linear model.

To test differences of cvGPP_{sat} between the age and nutrient availability classes, we used the Kruskal-Wallis rank sum test. Sites were divided by age class (young, middle aged and mature stands) according to the 33rd and 66th percentiles of the distribution of age. Nutrient availability classes were defined according to ref. ¹⁷ (low, medium and high).

The correlation between GPP_{sat} and climate variables was tested with distance correlation³³. Distance correlation is a measure of statistical dependence between random variables and here we tested the dependence between GPP_{sat} and temperature and WAI jointly.

Code availability. The analysis was conducted in R version 3.2.4 and the script of the analysis is available within the supplementary files of the paper.

Data availability. The authors declare that the data supporting the findings of this study are available within the Supplementary Information.

received 25 July 2016; accepted 9 December 2016;
published 23 January 2017

References

1. Ahlström, A. *et al.* The dominant role of semi-arid ecosystems in the trend and variability of the land CO₂ sink. *Science* **348**, 895–899 (2015).
2. Le Quéré, C. *et al.* Trends in the sources and sinks of carbon dioxide. *Nat. Geosci.* **2**, 831–836 (2009).
3. Luo, Y., Keenan, T. F. & Smith, M. Predictability of the terrestrial carbon cycle. *Glob. Change Biol.* **21**, 1737–1751 (2015).
4. Ma, S. Y., Baldocchi, D. D., Mambelli, S. & Dawson, T. E. Are temporal variations of leaf traits responsible for seasonal and inter-annual variability in ecosystem CO₂ exchange? *Funct. Ecol.* **25**, 258–270 (2010).
5. Reichstein, M., Bahn, M., Mahecha, M. D., Kattge, J. & Baldocchi, D. D. Linking plant and ecosystem functional biogeography. *Proc. Natl Acad. Sci. USA* **111**, 13697–13702 (2014).

6. Richardson, A. D., Hollinger, D. Y., Aber, J. D., Ollinger, S. V. & Braswell, B. H. Environmental variation is directly responsible for short- but not long-term variation in forest-atmosphere carbon exchange. *Glob. Change Biol.* **13**, 788–803 (2007).
7. Musavi, T. *et al.* The imprint of plants on ecosystem functioning: A data-driven approach. *Int. J. Appl. Earth Obs. Geoinform.* **43**, 119–131 (2015).
8. Xia, J. *et al.* Joint control of terrestrial gross primary productivity by plant phenology and physiology. *Proc. Natl Acad. Sci. USA* **112**, 2788–2793 (2015).
9. Musavi, T. *et al.* Potential and limitations of inferring ecosystem photosynthetic capacity from leaf functional traits. *Ecol. Evol.* **6**, 7352–7366 (2016).
10. Holling, C. S. Resilience and stability of ecological systems. *Annu. Rev. Ecol. System.* **4**, 1–23 (1973).
11. Jucker, T., Bouriaud, O., Avacaritei, D. & Coomes, D. A. Stabilizing effects of diversity on aboveground wood production in forest ecosystems: linking patterns and processes. *Ecol. Lett.* **17**, 1560–1569 (2014).
12. Garcia-Palacios, P., Maestre, F. T. & Gallardo, A. Soil nutrient heterogeneity modulates ecosystem responses to changes in the identity and richness of plant functional groups. *J. Ecol.* **99**, 551–562 (2011).
13. Von Oheimb, G. *et al.* Does forest continuity enhance the resilience of trees to environmental change? *PLoS ONE* **9**, e113507 (2014).
14. Kutsch, W. L. *et al.* in *Old-Growth Forests: Function, Fate and Value* (eds Wirth, C., Gleixner, G. & Heimann, M.) 57–79 (2009).
15. Herbst, M., Mund, M., Tamrakar, R. & Knohl, A. Differences in carbon uptake and water use between a managed and an unmanaged beech forest in central Germany. *Forest Ecol. Manage.* **355**, 101–108 (2015).
16. Brando, P. M. *et al.* Seasonal and interannual variability of climate and vegetation indices across the Amazon. *Proc. Natl Acad. Sci. USA* **107**, 14685–14690 (2010).
17. Fernandez-Martinez, M. *et al.* Nutrient availability as the key regulator of global forest carbon balance. *Nat. Clim. Change* **4**, 471–476 (2014).
18. Baldocchi, D. Breathing of the terrestrial biosphere: lessons learned from a global network of carbon dioxide flux measurement systems. *Austr. J. Bot.* **56**, 1–26 (2008).
19. Grömping, U. Relative importance for linear regression in R: the package relaimpo. *J. Stat. Software* **17**, 1–27 (2006).
20. Magnani, F. *et al.* The human footprint in the carbon cycle of temperate and boreal forests. *Nature* **447**, 848–850 (2007).
21. Urbanski, S. *et al.* Factors controlling CO₂ exchange on timescales from hourly to decadal at Harvard Forest. *J. Geophys. Res. Biogeosci.* **112**, G02020 (2007).
22. Bonan, G. B., Oleson, K. W., Fisher, R. A., Lasslop, G. & Reichstein, M. Reconciling leaf physiological traits and canopy flux data: use of the TRY and FLUXNET databases in the Community Land Model version 4. *J. Geophys. Res. Biogeosci.* **117**, G02026 (2012).
23. Medvigy, D., Jeong, S. J., Clark, K. L., Skowronski, N. S. & Schafer, K. V. R. Effects of seasonal variation of photosynthetic capacity on the carbon fluxes of a temperate deciduous forest. *J. Geophys. Res. Biogeosci.* **118**, 1703–1714 (2013).
24. Wirth, C. in *Old-Growth Forests: Function, Fate and Value* (eds Wirth, C., Gleixner, G. & Heimann, M.) 465–491 (2009).
25. Butterbach-Bahl, K. *et al.* *Nitrogen Processes in Terrestrial Ecosystems* (eds Sutton, M. A. *et al.*) 99–125 (Cambridge Univ. Press, 2011).
26. Sutton, M. A. *et al.* *The European Nitrogen Assessment: Sources, Effects and Policy Perspectives* (eds Sutton, M. A. *et al.*) (Cambridge Univ. Press, 2011).
27. Yang, Y. H., Luo, Y. Q. & Finzi, A. C. Carbon and nitrogen dynamics during forest stand development: a global synthesis. *New Phytol.* **190**, 977–989 (2011).
28. Grossiord, C., Granier, A., Gessler, A., Jucker, T. & Bonal, D. Does drought influence the relationship between biodiversity and ecosystem functioning in boreal forests? *Ecosystems* **17**, 394–404 (2014).
29. Del Rio, M., Schütze, G. & Pretzsch, H. Temporal variation of competition and facilitation in mixed species forests in Central Europe. *Plant Biol.* **16**, 166–176 (2014).
30. Becknell, J. M. & Powers, J. S. Stand age and soils as drivers of plant functional traits and aboveground biomass in secondary tropical dry forest. *Canadian J. Forest Res.* **44**, 604–613 (2014).
31. Coursolle, C. *et al.* Influence of stand age on the magnitude and seasonality of carbon fluxes in Canadian forests. *Agric. Forest Meteorol.* **165**, 136–148 (2012).
32. Luyssaert, S. *et al.* Old-growth forests as global carbon sinks. *Nature* **455**, 213–215 (2008).
33. Szekely, G. J., Rizzo, M. L. & Bakirov, N. K. Measuring and testing dependence by correlation of distances. *Ann. Stat.* **35**, 2769–2794 (2007).
34. Reichstein, M. *et al.* On the separation of net ecosystem exchange into assimilation and ecosystem respiration: review and improved algorithm. *Glob. Change Biol.* **11**, 1424–1439 (2005).
35. Tramontana, G. *et al.* Predicting carbon dioxide and energy fluxes across global FLUXNET sites with regression algorithms. *Biogeosci. Discuss.* **2016**, 1–33 (2016).
36. Law, B. E. *et al.* *Terrestrial Carbon Observations: Protocols for Vegetation Sampling and Data Submission* (FAO, 2008).
37. DiMiceli, C. M. *et al.* *Annual Global Automated MODIS Vegetation Continuous Fields (MOD44B) at 250 m Spatial Resolution for Data Years Beginning Day 65, 2000 - 2010, Collection 5 Percent Tree Cover* (Univ. Maryland, 2011); <http://glcf.umd.edu/data/vcf/>
38. Simard, M., Pinto, N., Fisher, J. B. & Baccini, A. Mapping forest canopy height globally with spaceborne lidar. *J. Geophys. Res. Biogeosci.* **116**, G04021 (2011).
39. Pinty, B. *et al.* Retrieving surface parameters for climate models from Moderate Resolution Imaging Spectroradiometer (MODIS)-Multiangle Imaging Spectroradiometer (MISR) albedo products. *J. Geophys. Res. Atmos.* **112**, D10116 (2007).
40. Schaaf, C. B. *et al.* First operational BRDF, albedo nadir reflectance products from MODIS. *Remote Sens. Environ.* **83**, 135–148 (2002).
41. Pinty, B. *et al.* Evaluation of the JRC-TIP 0.01 degrees products over a mid-latitude deciduous forest site. *Remote Sens. Environ.* **115**, 3567–3581 (2011).
42. Gilmanov, T. G. *et al.* Gross primary production and light response parameters of four Southern Plains ecosystems estimated using long-term CO₂-flux tower measurements. *Glob. Biogeochem. Cycles* **17**, 1071 (2003).
43. Venables, W. N. & Ripley, B. D. *Modern Applied Statistics with S* (Springer, 2002).

Acknowledgements

From Max-Planck Institute for Biogeochemistry we thank U. Weber, M. Jung for providing data, and K. Morris and R. Nair for a language check. We thank P. Jassal from the University of British Columbia and Jens Schumacher from University of Jena for their helpful comments. The authors T.M., M.M., M.D.M., J.K., C.W. and M.R. affiliated with the MPI BGC acknowledge funding by the European Union's Horizon 2020 project BACI under grant agreement no. 640176. This work used eddy covariance data acquired and shared by the FLUXNET community, including these networks: AmeriFlux, AfriFlux, AsiaFlux, CarboAfrica, CarboEuropeIP, CarboItaly, CarboMont, ChinaFlux, Fluxnet-Canada, GreenGrass, ICOS, KoFlux, LBA, NECC, OzFlux-TERN, TCOS-Siberia and USCCC. The ERA-Interim reanalysis data are provided by ECMWF and processed by LSCE. The FLUXNET eddy covariance data processing and harmonization was carried out by the European Fluxes Database Cluster, AmeriFlux Management Project, and Fluxdata project of FLUXNET, with the support of CDIAC and ICOS Ecosystem Thematic Center, and the OzFlux, ChinaFlux and AsiaFlux offices. T.M. acknowledges the International Max Planck Research School for global biogeochemical cycles.

Author contributions

T.M. wrote the manuscript and performed the analysis. T.M., M.M., M.D.M. and M.R. designed the study. M.M., M.D.M., M.R., J.K., I.J., A.K., A.C., C.W., T.A.B. and A.V. discussed the interpretation of the results. M.M., M.D.M., M.R., J.K., C.W., T.A.B., A.C., A.K., D.L. and O.R. contributed significantly to editing the paper. S.R., R.T. and D.G. contributed to editing the paper. T.A.B., I.J., A.K., D.L., O.R., A.V., S.R., A.C., H.K. and T.F. contributed data.

Additional information

Supplementary information is available for this paper.

Reprints and permissions information is available at www.nature.com/reprints.

Correspondence and requests for materials should be addressed to T.M.

How to cite this article: Musavi, T. *et al.* Stand age and species richness dampen interannual variation of ecosystem-level photosynthetic capacity. *Nat. Ecol. Evol.* **1**, 0048 (2017).

Competing interests

The authors declare no competing financial interests.